Fishing Harbor, Homer, AK

PART IV

COASTAL ESTUARINE AND ENVIRONMENTAL PROBLEMS

Boardwalk, Cape May, N.J.

CHAPTER ONE HUNDRED NINETY EIGHT

EVOLUTION OF INTERFACIAL WAVES ALONG AN UNSTEADY SALT WEDGE

by

Wataru Nakano[*] and Isao Yakuwa[**]

ABSTRACT

Field measurements of the receding salt wedge were made at the mouth of the Ishikari River in October 1981. The gradually growing interfacial waves and the diffusion pattern of salinity are visualized by the Ultrasonic Method. The evolution mechanisms of waves are analysed in detail by calculating the power spectra of wave records. It is pointed out that the wave breaking, the wave-eddy interaction and the nonlinearity of waves are factors dominating the evolution. The nonlinear property of interfacial waves is studied further by watertank experiments.
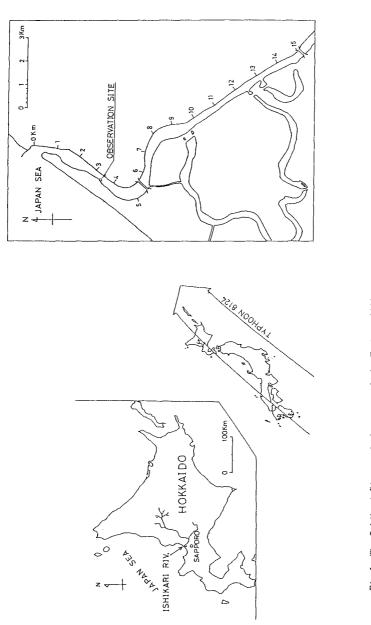
INTRODUCTION

Because a salt wedge influences the flow structure and water quality in the estuary, many studies about it have been carried out by various research methods. The theoretical study and laboratory experiment have found out the importance of internal waves in the dynamics of the stratified shear flow[8]. The results of field observations, however, shows that in the steady state of the salt wedge the interfacial waves are not the factor controlling the diffusion process because the amplitudes of interfacial waves are small under this condition. Do the interfacial waves, on the other hand, play an important role in the unsteady salt wedge? Regrettably, there is not enough observational research of the unsteady salt wedge. So we planned to observe the interfacial waves along the unsteady salt wedge in the Ishikari River.
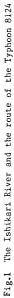
The Ishikari River, which has a length of 262 km, flows through the Ishikari Plane and pours into the Japan Sea (Fig. 1). The normal discharge of this river is about 300 m³/sec. Because the critical discharge Q_c for the intrusion of the salt wedge into the river mouth is about 600 m³/sec [3], the salt wedge steadily lies in the water course to a point about 8 km upstream from the river mouth under the usual river flow.

----

[*] Postgraduate Student, Division of Applied Physics,
    Hokkaido University, Sapporo 060, Japan.
[**] Professor, Department of Engineering Science,
    Hokkaido University, Sapporo 060, Japan.

Fig.2 Location map

Fig.1 The Ishikari River and the route of the Typhoon 8124

From October 22 to October 23, 1981, a severe 960-millibar typhoon (the Typhoon 8124) hit and passed through the Japanese Islands as shown in Fig.1. Because of the heavy rain brought about by this typhoon in the drainage basin of the Ishikari River, the river discharge increased from 300 to 2,250 m^3/sec beyond the critical value Q_c. On these two days, we had a chance to observe the interfacial gravity waves propagating along the interface of the unsteady salt wedge. The purpose of this paper is to report the observational results and to make clear the evolution mechanisms of the interfacial waves along an unsteady salt wedge.

FIELD OBSERVATION

The estuary of the Ishikari River is drawn in Fig.2. The observation was conducted on a pier which locates 3.5 km upstream from the river mouth. As shown in Fig.3, the displacement of interface was measured with two echo-sounder transducers, No.1 and No.2. No.1 was settled facing downwards slightly under the water surface, whereas, No.2 was settled facing upwards on the riverbed to record the both of the water level and the displacement of interface.
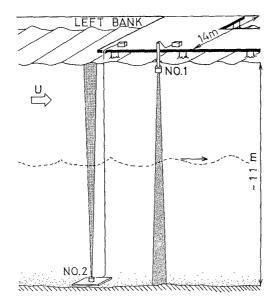

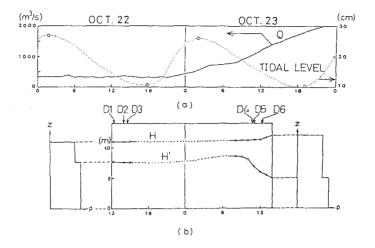Fig.3 Pier station and two echo-sounder transducers

Fig.4 Hydraulic conditions. (a)History of river discharge Q and tidal
level. (b)History of the level of surface H and interface H'.

The hydraulic conditions during the observation are summarized in
Fig.4. Fig.4(a) shows the history of the river discharge and the
tidal level. The latter has been observed at Otaru Port which locates
about 30 km west from the river mouth. Fig.4(b) shows the history of
the surface level H and the interface level H' measured at the
station. After a weak tidal motion, the interface level H' begins to
lower rapidly at 9:00 on October 23 according to the increase of river
discharge. The echo-sounder measurement was performed from 11:00 to
15:00 on October 22 and from 8:00 to 13:00 on October 23. The six
series of wave records were sampled at short time intervals numbered
from D1 to D6 in Fig.4(b). Because we had to use the clearer image to
analyse the data accurately, the data D1, D2 and D3 are sampled from
the chart of echo-sounder No.1, and the data D4, D5 and D6 are sampled
from that of No.2.

The charts D1, D2 and D3 in Fig.5(a) were recorded on October 22.
At these stages the river charged almost steady discharge of 350
m^3/sec that was fairly smaller than the critical value Q_c of 600
m^3/sec. The depth at the observation point was about 11 m. The river
bed cannot be seen in these figures. The chart D1 shows that several
waves of small amplitude are intermittently propagating along the
interface lying at 3.5 m depth. The wave height and the wave period
are about 30 cm and 18 sec respectively. In the stage of D2, the
waves are going through more frequently, and in the stage of D3, the
wave height attains to 50 cm and the waves become short-crested. It

will also be noted that the wave breaking and the destruction of
interface are taking place.

On October 23, the river discharge abruptly increased beyond the
critical discharge Q_c. The recorded charts are shown in Fig.5(b). D4
shows the large scale random and modulated waves, which are
propagating along the interface lying at 6 m depth and are causing
violent wave breaking. It may be seen that the intrefacial waves are
playing an important role in salinity diffusion. The wave height is
about 80 cm and the wave period is obtained as about 21 sec. The waves
shown in D5 have longer period of 30 sec and waves are propagating
more periodically. After 85 minutes, in the stage shown in D6, the
waves recur to the modulated state and the wave period lengthens up to
40 sec and the wave height attains to 2 m.

SPECTRAL ANALYSIS

To make clear the evolution mechanism of interfacial waves, we
calculated the power spectra of recorded waves, which are shown in
Fig.6. Each spectrum was calculated by FFT method with 512 data
sampled from the recorder charts shown in Fig.5(a) and (b). In each
figure the spectrum is drawn with a solid line. Further, the spectrum
of preceding step is drawn with a broken line for a convenience of
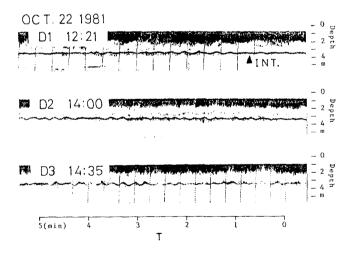comparison.

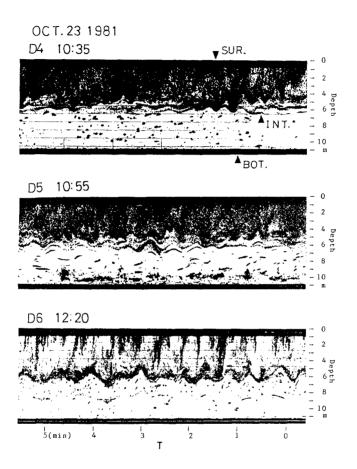Fig.5(a) Echo-sounding images recorded on Oct. 22.

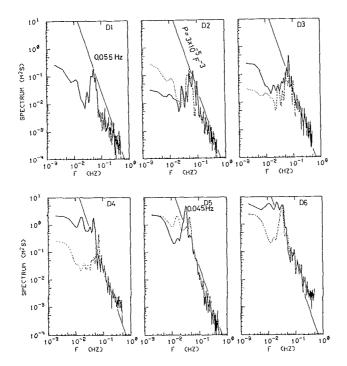Fig.5(b)   Echo-sounding images recorded on Oct. 23.

Fig.6 Power spectra of interfacial waves (solid lines). The broken line in each figure represents the spectrum of the preceding step.

Corresponding to the mean wave period of 18 sec shown in the chart of Fig.5(a), the spectrum of D1 has a distinct spectral peak at 0.055 Hz. In this stage, the power spectra in higher frequency range decreases with frequency f more dully than f^{-3}. After this stage the spectrum approachs a saturated spectral form in high frequency range which decreases with f as f^{-3} as shown in D2 and D3. Spectral form of this type has been observed in the spectra of ocean internal waves [2] and theoretical explanation of this spectral form has been proposed by Phillips[6]. Phillips[6] derived the f^{-3}-spectrum by assuming the local breakdown of internal waves caused by shear stress in wave motion. Therefore, the growth of spectrum from D1 to D3 indicates that the local breakdown process of the interfacial waves is beginning at this stage. The local breakdown process must be the mechanism controlling the earlier stage of evolution.

Though the f^{-3}-spectrum in high frequency range is maintained also in the later stage, another feature is noted in D4, D5 and D6 of

Fig.6. The spectrum of D4 has one small peak and two larger peaks.
The small one grows the narrow dominant peak in D5. After this stage,
the lower side components of this peak grow the new maximum peak in
D6. This result indicates that in these stages the waves go through a
modulation–demodulation cycle and the frequency of dominant components
shifts to the lower frequency side. These phenomena are explained in
the following section.

TWO MECHANISMS OF EVOLUTION

The process of modulation–demodulation and frequency downshift of
interfacial waves can be interpreted by assuming two different
mechanisms:

The first mechanism is an interaction between the interfacial
waves and turbulent eddies in the upper layer. The upper figure of
Fig.7 is same as the chart D5 of Fig.5(a). The diffusion patterns of
salinity in the upper layer indicates the existence of large scale
turbulent eddies in this layer. It seems that these eddies have a
mean vertical scale comparable to the thickness of the upper layer and
have a mean period comparable to that of the interfacial waves. These
eddies will cause the pressure disturbance along the interface. This
pressure disturbance will supply its energy to the interfacial waves
of the same horizontal scale as that of eddies as shown in Fig.8(a).
By the way, the scales of the eddies are restricted under the
thickness of the upper layer, which increases with discharge. It
follows that the length and period of interfacial waves increase as
the discharge increases. Further, if the horizontal scales of waves
and eddies are mismatched, the wavetrain will modulated as shown in
Fig.8(b). The cycle of matching and mismatching of two scales will
leads the waves to the process of modulation–demodulation.

The second mechanism is based on the nonlinearity of interfacial
waves. Both of the modulation–demodulation cycle and the downshift of
frequency were observed by Lake et al.[5] in the laboratory experiment
of finite amplitude surface waves. The former phenomenon was
explained by the nonlinear Schrödinger equation for complex amplitude
$A(x,t)$:

$$i(\frac{\partial A}{\partial t} + \frac{d\omega}{dk}\frac{\partial A}{\partial x}) + \mu\frac{\partial^2 A}{\partial x^2} + \nu|A|^2 A = 0 , \qquad (1)$$

where k and ω are carrier wave number and carrier frequency
respectively, and μ and ν are coefficients characteristic of the
system. The displacement $\eta(x,t)$ is related to $A(x,t)$ by

$$\eta(x,t) = A(x,t)\exp[i(kx-\omega t)] + c.c. , \qquad (2)$$

The nonlinear modulational instability described by the equation(1)
is summarised as follows: The nonlinear plane wave shown in Fig.9(a)
is unstable to small disturbances in the form of a pair of side–band
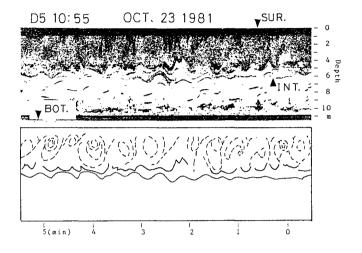modes; at initial stage the modulational disturbances grow

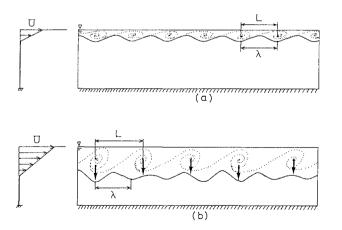Fig.7   Large scale turbulent eddies in the upper layer.

(a)

(b)

Fig.8   Eddy-wave interaction

exponentially with time; the long-time evolution is completely
recursive and the side-band modes are symmetric throughout the
evolution as shown in Fig.9(c)-(e). In the experiments performed by
Lake et al.[5], however, the side-band components grew asymmetrically
as shown in Fig.9(f)-(h) and the downshift of wave frequency was
observed.

    At present stage, the data is not sufficient to conclude this
problem. In the following chapter, the nonlinear instability of
interfacial waves is investigated by laboratory experiment.

                              EXPERIMENT

    The apparatus used is depicted in Fig.10. The experiments were
performed in the 25cmx50cmx600 cm watertank in which a two-layer
density stratification had been formed by fresh water (specific
gravity of 1.004) and salt water (specific gravity of 1.061). The
thickness of fresh water layer was 20.5 cm and that of salt water
layer was 19.5 cm. Modulated waves were generated by a wave maker at
one end of the tank and absorbed by a wave absorbing beach at the
opposite end. The evolution of waves was measured with seven infrared
type wave amplitude gauges located at the stations 0.5m, 1m, 2m, 3m,
4m, 5m, and 5.4 m downstream of the wave maker. The wave gauges are
similar to that imploved by Koop et al.[4]. The data measured at all
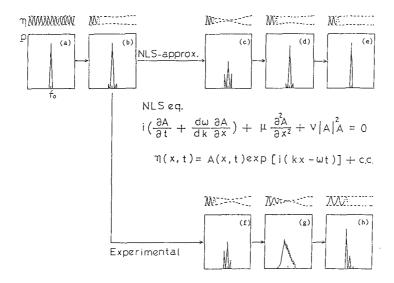stations were recorded on the chart of multi-pen recorder and the data

Fig.9 Nonlinear modulational instability of surface waves.
Theoretical prediction based on the nonlinear Schrödinger equation and
the experimental result of Lake et al.[5].

measured at stations 0.5m, 1m, 2m and 3m were recorded also in a 4-ch
FM data-recorder to calculate power spectra of interfacial waves.

It is well known that wave train is unstable to modulational
disturbance if the coefficients of the nonlinear Schröbdinger
equation(1) μ and ν satisfy the inequality:

$$\mu\nu > 0 \qquad\qquad\qquad (3)$$

Tanaka[7] derived formulae which express the coefficients
characteristc of interfacial waves as functions of the wave number,
the density of two fluids and the thickness of each layer. Since the
wave length is 31 cm in our experiments, the coefficients are
calculated as $\mu=8.5$ $cm^2 sec^{-1}$ and $\nu =0.049$ $sec^{-1} cm^{-2}$ by Tanaka's
formulae[7]. Because $\mu\nu \approx 0.42$ $sec^{-2} > 0$, the modulational instability
can be expected under this condition. The growth of modulational
disturbance, however, depended on the strength of initial modulation
given by the wave generator because the viscosity dumped the power of
small amplitude disturbance. For example, the waves which had not
been modulated at the wave generator were never modulated throughout
the propagation even when it satisfied the instability condition (3).

When the waves had been initially modulated, modulaton-
demodulation cycles were found, as shown in Fig.11. Initially
modulated waves have large modulation amplitude at the station of 0.5
m, and become almost unmodulated state at 1.0 m. At the station of
2.0 m, strong modulation appears for the second time, and at 3.0 m the
modulation becomes relatively weak. After these stages, waves are
separated into many wave pulses. This figure resembles that measured
by Lake et al.[5].

To examine whether the recurrence observed in the experiment is a
nonlinear phenomenon or not, we calculated power spectra of the data
measured at the stations 0.5 m, 1.0 m, 2.0 m and 3.0 m. The
calculated spectra are shown in Fig.12. In Fig.12(a) the spectrum has
one large peak at frequency 0.36 Hz and two smaller side-band peaks at
frequencys 0.36 ± 0.039 Hz. These side-band components are severely
modulating the carrier waves in this stage, but they decrease in the
stage of Fig.12(b) showing that the modulation are weaken. In the
following stages shown in Figs.11(c) and (d), the lower side-band
components increase a little as shown in Fig.12(d), whereas the
fundamental components and higher side-band components decrease, in
consequence, it may be regarded that the lower side-band components
are growing in relative sense. This mutual exchange of spectral power
between different modes indicates that the modulation-demodulation
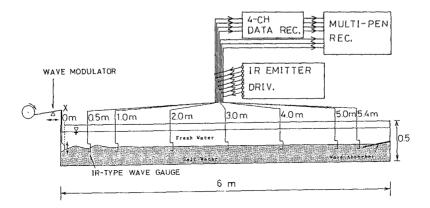process observed in the experiment is the nonlinear process in
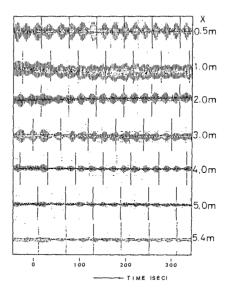essence.

Fig.10 Experimental apparatus.

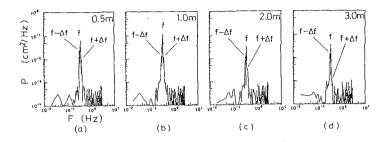Fig.11 Wave shape observed at seven points.

Fig.12 Power spectra.

CONCLUSIONS

Based on the results of the field measurement of an unsteady salt wedge, it is concluded that:

1. When the river discharge increases beyond a critical value, the salt wedge recedes and interfacial waves of considerable amplitude appear along the interface of fresh and salt water.

2. These interfacial waves grow through following two stages:

   In the earlier stage, the interfacial waves of small amplitude grow and become short-crested. The growth of waves in this stage is controlled by the mechanism of local breakdown discovered by Phillips[6].

   In the later stage the violent wave breaking begins and the interfacial waves become an important factor of salinity diffusion.

3. The process of modulation-demodulation and frequency downshift observed in the later stage may be interpreted by either or both of the following mechanisms: (a)Interaction between interfacial waves and turbulent eddies in the fresh water layer, (b)Nonlinear modulation mechanism in large amplitude interfacial waves. But at present stage, the data are not sufficient to conclude.

4. In laboratory scale, the nonlinear modulational instability takes place also in interfacial waves if the initial modulation is sufficiently strong.

REFERENCES

1. Benjamin, T. B. and J. E. Fair, 1967, "The disintegration of wave trains on deep water, Part 1. Theory," J. Fluid Mech., Vol.27, 417–430.

2. Brekhovskikh, K., K. V. Konjaev, K. D. Sabinin and A. N. Serikov, 1975, "Short-period internal waves in the sea," J. Geophys. Res., Vol.80, No.6, 856–864.

3. Fukushima, H., M. Kashiwamura and I. Yakuwa, 1966, "Studies on salt wedge by ultrasonic method," Proc. Coastal Engg., 1435–1447.

4. Koop, C. G., H. Rungaldier and J. D. Sherman, 1979, "Infrared optical sensor for measuring internal interfacial wave motions," Rev. Sci. Instrum., Vol.50, No.1, 20–23.

5. Lake, B. M., H. C. Yuen, H. R. Rungaldier and W. E. Ferguson, 1977, "Nonlinear deep-water waves: theory and experiment, Part 2. Evolution of continuous wave train," J. Fluid Mech., Vol.83, 49–74.

6. Phillips, O. M., 1977, "The dynamics of the upper ocean," 2nd ed., Cambridge, Cambridge University Press.

7. Tanaka, M., 1982, "Nonlinear self-modulation of interfacial waves," J. Phys. Soc. Jpn., Vol.51, No.6, 2016–2023.

8. Thorpe, S. A., 1971, "Experiments on the instabillity of stratified shear flows: miscible fluids," J. Fluid Mech., Vol.46, 299–319.